PAPER

Geodesic acoustic modes in tokamak plasmas with anisotropic distribution and a radial equilibrium electric field

Plasma Sci. Technol. **20** (2018) 085101 (6pp) https://doi.org/10.1088/2058-6272/aabc5c

Geodesic acoustic modes in tokamak plasmas with anisotropic distribution and a radial equilibrium electric field

Yue MING (明玥)[1,2,3], Deng ZHOU (周登)[1,3] and Wenjia WANG (王文家)[1,2,3]

[1] Institute of Plasma Physics, Chinese Academy of Sciences, Hefei 230031, People's Republic of China
[2] University of Science and Technology of China, Hefei 230026, People's Republic of China
[3] Center for Magnetic Fusion Theory, Chinese Academy of Sciences, Hefei 230031, People's Republic of China

E-mail: mingyue@ipp.ac.cn

Received 5 January 2018, revised 8 April 2018
Accepted for publication 8 April 2018
Published 6 July 2018

Abstract

The dispersion relation of standard geodesic acoustic modes in tokamak plasmas with anisotropic distribution and a radial equilibrium electric field is derived and analyzed. Both frequencies and damping rates increase with respect to the poloidal Mach number which indicates the strength of the radial electric field. The strength of anisotropy is denoted by the ratio of the parallel temperature ($T_{\|}$) to the perpendicular temperature ($T_{\perp}$). It is shown that, when the parallel temperature is lower than the perpendicular temperature, the enhanced anisotropy tends to enlarge the real frequency but reduces the damping rate, and when the parallel temperature is higher than the perpendicular temperature, the effect is opposite. The radial equilibrium electric field has stronger effect on the frequency and damping rate for the case with higher parallel temperature than the case with higher perpendicular temperature.

Keywords: geodesic acoustic mode, anisotropy, equilibrium flow

1. Introduction

Zonal flows (ZFs), which are electrostatic symmetric band-like shear flows in toroidal plasmas, have caught great attention due to their important roles of regulating the plasma turbulence and the resultant transport [1–3]. A number of theoretical researches and experiments have been devoted to the new paradigm which regards plasma turbulence as a system of drift waves and ZFs. In tokamak devices, ZFs have two branches: the low frequency zonal flow with $\omega \sim 0$ and the geodesic acoustic mode (GAM) with $\omega \sim c_s/R$, where c_s is the sound speed. GAMs, usually as an electrostatic acoustic mode due to the geodesic curvature, have been investigated for several decades since first predicted by Winsor *et al* [4]. They have been studied by many researchers from different aspects.

In theory, Zhou [5] investigated the GAM with a radial equilibrium electric field and found that the real frequency and damping rate do increase with the increasing poloidal Mach number. He also investigated the effect of magnetic perturbation on GAMs [6]. Wahlberg [7] investigated the effect of toroidal rotation on GAMs, finding a new GAM with much lower frequency produced by the rotation. Xie *et al* [8] analyzed the influence of the poloidal rotation on the collisional damping of GAMs. GAMs are usually excited by self-interation of turbulence in toroidal devices. Itoh *et al* studied the excitation of GAMs through the poloidally nonsymmetric radial transport caused by turbulence [9]. Chakrabarti *et al* investigated the nonlinear excitation of GAMs by diverse drift waves through three wave coupling [10]. Sasaki *et al* analyzed the self-nonlinear interaction of GAM, showing nonlinearity effect of density, parallel velocity and Reynolds stress on the saturation level in different orders [11]. In a recent experiment, the characteristics and scaling properties of GAMs have been investigated on JET [12], the driving of GAMs by turbulence dominant over the damping rate was confirmed.

Normally the studies of GAMs are performed in isotropic equilibria, like for ohmic discharges. The anisotropy occurs only in first δ-order ($\partial f_0/\partial \mu = \mathcal{O}(\delta)$), where $\delta = \rho/L$ with ρ

the gyro-radius and L the equilibrium scale, and is usually neglected in the analysis. However, with the application of diverse auxiliary heating methods in modern tokamak devices, like neutral beam injection, ion cyclotron resonance heating, etc, the isotropic assumption may not always persist. The investigation of the anisotropic effect for tokamak plasmas has been in progress for a long time [13–17]. Heidbrink and Sadler [18] analyzed the behavior of fast ions, and found that the distribution was quite anisotropic during ICRF minority heating. Ivanov *et al* [15], using the SPIDER code, derived the axisymmetric plasma equilibrium equation with arbitrary rotation and anisotropic pressure. Ren [16] investigated the influence of anisotropy on GAMs with a toroidal rotation, and found that the degree of anisotropy did always enlarge the GAM frequency. With high power auxiliary heating, it is possible to excite the energetic particle-induced geodesic acoustic mode (EGAM), which was first observed in the experiment of DIII-D [19]. Fu [20] analyzed the excitation of EGAM, finding the frequency and structure determined nonperturbatively by energetic particle kinetic effects. Berk and Zhou [21] investigated the fast excitation of EGAM, finding a new mechanism which is crucially related to the loss region. Qiu *et al* [22] investigated the excitation of EGAM, coupling with the GAM continuous spectrum. Sasaki *et al* [23] analyzed EGAM, finding a new branch due to the magnetic drift resonance.

In this work, we investigate the GAMs in a tokamak with a radial equilibrium electric field and anisotropic ion distributions. Usually in tokamak plasmas, there is a radial equilibrium electric field, especially near the edge of plasmas. As a consequence, sometimes an equilibrium poloidal mass flow may appear [24, 25]. Some investigations have addressed the effect of plasma poloidal flows or radial equilibrium electric fields on the characteristics of GAMs. The frequency of standard GAMs had a significant up-shift with the increasing poloidal rotation velocity or field strength [5, 26]. Elfimov *et al* [24] revealed that a low frequency branch induced by the rotation exists when the energy equation was taken into account. The Alfvenic continuum of a poloidally rotating plasma was investigated by Lakhin and Ilgisonis [27]. However, most of the researches are considered in the isotropic condition. With the application of auxiliary heating methods in modern fusion research, it is necessary to investigate the anisotropic condition, finding the effect of coexistence of the radial equilibrium electric field and anisotropic distribution.

We solve the gyro-kinetic equation for an axisymmetric electrostatic perturbation with small side-band included, the dispersion relation is then obtained by quasi-neutrality conditions. The magnetic perturbation, which is related to the finite beta effect, is not considered in the present work. It is straightforward to include the magnetic component, but the process will be very complicated. Usually, energetic particles will appear in experiments with high power auxiliary heating in addition to the anisotropic equilibrium distribution. It is interesting to study the EGAM with the background anisotropic distribution, but it is beyond the scope of the present work.

In the following, taking into account the anisotropy and a radial electric field, we derive the dispersion relation in section 2. Considering the standard GAMs, which means the normalized frequency $\xi \gg 1$ (where $\xi = qR\omega/v_T$), we numerically solve the dispersion relation and get the profiles of the mode frequency and the damping rate in section 3. We give an analysis on the mode frequency and damping rate with respect to the radial electric field and the degree of the anisotropy. The conclusion and discussion are presented in section 4.

2. Derivation of the dispersion relation

In this section, we derive the dispersion relation for a large aspect ratio tokamak with circular cross section. The coordinates $(r,\ \theta,\ \phi)$ here indicate the radial variable, poloidal angle, and toroidal angle, respectively. The axisymmetric magnetic field here is $\vec{B} = \nabla\phi \times \nabla\psi + B_T R\nabla\phi$ with $R = R_0 + r\cos\theta$ and the radial electric field is $\vec{E}_r = -\nabla\Phi = -\Phi'\nabla\psi$ where ψ labels a magnetic surface.

We assume the ion equilibrium distribution with anisotropy as (the electrons should have the same distribution function in order to satisfy the quasi-neutrality condition)

$$f_{0\mathrm{i}} = \frac{N(\psi)}{\pi^{3/2}v_{T_\mathrm{i}}^3}\mathrm{e}^{-\left(\frac{E_\mathrm{i}}{T_{E_\mathrm{i}}}+\frac{\mu_\mathrm{i}B}{T_{\mu_\mathrm{i}}}\right)}, \tag{1}$$

where $N(\psi)$ is the density of ion, $v_{T_\mathrm{i}} = (2T_{E_\mathrm{i}}/m_\mathrm{i})^{1/2}$, $E_\mathrm{i} = m_\mathrm{i}v^2/2 + q_\mathrm{i}\Phi$ and magnetic moment $\mu_\mathrm{i} = m_\mathrm{i}v_\perp^2/(2B)$. The equilibrium distribution is required to satisfy the condition $\hat{b}\cdot\nabla f_{0\mathrm{i}} = 0$ where $\hat{b}$ is the unit vector in the direction of the magnetic field. We can get $\hat{b}\cdot\nabla(B/T_{\mu_\mathrm{i}}) = 0$ which means the T_{μ_i} is not just the function of magnetic surface. It indicates $T_{\mu_\mathrm{i}} = T_{\mu_\mathrm{i}}(\psi,\ \theta) \propto B$.

Using the equilibrium distribution, the equilibrium density of ion is obtained as

$$n_{0\mathrm{i}} = \int f_{0\mathrm{i}}\,\mathrm{d}^3v = N(\psi)\mathrm{e}^{-\frac{q_\mathrm{i}\Phi}{T_{E_\mathrm{i}}}}\frac{1}{1 + T_{E_\mathrm{i}}/T_{\mu_\mathrm{i}}}. \tag{2}$$

Defining $\tau = T_{E_\mathrm{i}}/T_{\mu_\mathrm{i}}$ which represents the degree of the anisotropy, the ion equilibrium distribution can be written as

$$f_{0\mathrm{i}} = \frac{N(\psi)}{\pi^{3/2}v_{T_\mathrm{i}}^3}\mathrm{e}^{-\left(\frac{E_\mathrm{i}}{T_{E_\mathrm{i}}}+\frac{\mu_\mathrm{i}B}{T_{\mu\mathrm{i}}}\right)} = \frac{n_{0\mathrm{i}}(1+\tau)}{\pi^{3/2}v_{T_\mathrm{i}}^3}\mathrm{e}^{-\left(\frac{m_\mathrm{i}v^2}{2T_{E_\mathrm{i}}}+\frac{\mu_\mathrm{i}B}{T_{\mu_\mathrm{i}}}\right)}. \tag{3}$$

The parallel and perpendicular temperatures can be written as

$$T_\parallel = \frac{1}{n_0(\psi,\ \theta)}\int m_\mathrm{i}v_\parallel^2 f_{0\mathrm{i}}\,\mathrm{d}^3v = T_{E_\mathrm{i}} \tag{4}$$

and

$$T_\perp = \frac{1}{n_0(\psi,\ \theta)}\int\frac{1}{2}m_\mathrm{i}v_\perp^2 f_{0\mathrm{i}}\,\mathrm{d}^3v = \frac{T_{E_\mathrm{i}}}{1+\tau}. \tag{5}$$

From equations (4) and (5), the term $1 + \tau = T_\parallel/T_\perp$. We note that the parameter $T_\parallel/T_\perp$ is not only a flux function but also depends on the poloidal angle. However, for a large aspect ratio tokamak, the dependence on the poloidal angle is weak such that we can take the flux averaged values in numerical evaluations.

In order to satisfy the quasi-neutrality condition, electrons should have the similar distribution, but temperatures need not be the same. Taking equations (4) and (5) into the equilibrium distribution function, one can obtain the same form of the exponent which indicates the anisotropy as that in [13].

The total distribution function contains two parts: the equilibrium part and the perturbation part. It can be written as $f_\alpha = f_{0\alpha} + \delta f_\alpha$ where $\alpha = \mathrm{i(e)}$. The perturbation distribution can be written as [28]

$$\delta f_\alpha = \delta h(\vec{R}, t) + q_\alpha \delta\Phi(\vec{r}, t)\frac{\partial f_{0\alpha}}{\partial E} + \frac{q_\alpha}{B}\frac{\partial f_{0\alpha}}{\partial \mu} \times[1 - J_0(k_\perp \rho_\alpha)\mathrm{e}^{-\mathrm{i}\vec{k}_\perp\cdot\vec{\rho}_\alpha}]\delta\Phi(\vec{r}, t), \tag{6}$$

where $\delta\Phi$ is the perturbed electrostatic potential, J_0 is the zero-order Bessel function and $\rho_\alpha = v_\perp m_\alpha/(q_\alpha B)$ is the gyroradius. The non-adiabatic perturbation δh satisfies the gyrokinetic equation

$$\frac{\partial \delta h}{\partial t} + (v_\parallel \hat{b} + \vec{v}_\mathrm{E} + \vec{v}_\mathrm{D})\cdot\frac{\partial \delta h}{\partial \vec{R}} = -\frac{\mathrm{i}\omega q_\alpha}{T_{E_\alpha}} J_0(k_\perp\rho_\alpha)\delta\Phi(\vec{R}, t) f_{0\alpha}, \tag{7}$$

where $\vec{v}_\mathrm{E} = \vec{E}\times\vec{B}/B^2 \cong -\Phi' q^{-1} r\hat{\theta}$ is the electric drift velocity, $\vec{R} = \vec{r} - \vec{\rho}_\alpha$ is the guiding center, $\vec{v}_\mathrm{D} = -\hat{v}_\mathrm{D}\sin\theta\hat{r} - \hat{v}_\mathrm{D}\cos\theta\hat{\theta}$ is the magnetic drift with $\hat{v}_\mathrm{D} = (v_\parallel^2 + v_\perp^2/2)/(\Omega_\alpha R)$ and $\Omega_\alpha = q_\alpha B/m_\alpha$.

The perturbations are expanded in harmonic forms

$$\delta\Phi = \sum_{l=0,\pm1,\cdots}\Phi_l \exp[-\mathrm{i}(\omega t - k_r x - l\theta)], \tag{8a}$$

$$\delta h = \sum_{l=0,\pm1,\cdots}\delta h_l \exp[-\mathrm{i}(\omega t - k_r x - l\theta)]. \tag{8b}$$

Substituting equations (8*a*) and (8*b*) into equation (7) and neglecting high-order harmonics components with $|l| > 2$, one can obtain

$$\omega\delta h_0 + \frac{\mathrm{i}\omega_\mathrm{d}}{2}(\delta h_{+1} - \delta h_{-1}) = \frac{\omega q_\alpha}{T_{E_\alpha}} J_0\Phi_0 f_{0\alpha}, \tag{9a}$$

$$(\omega - \omega_t)\delta h_{+1} - \frac{\mathrm{i}\omega_\mathrm{d}}{2}\delta h_0 = \frac{\omega q_\alpha}{T_{E_\alpha}} J_0\Phi_{+1} f_{0\alpha}, \tag{9b}$$

$$(\omega + \omega_t)\delta h_{-1} + \frac{\mathrm{i}\omega_\mathrm{d}}{2}\delta h_0 = \frac{\omega q_\alpha}{T_{E_\alpha}} J_0\Phi_{-1} f_{0\alpha}, \tag{9c}$$

where $\omega_\mathrm{d} = k_r\hat{v}_\mathrm{D}$ and $\omega_t = (v_\parallel + \hat{v}_\mathrm{E})/qR$, with $\hat{v}_\mathrm{E} = R\Phi'$. As $\omega_\mathrm{d}/\omega \sim k_r\rho_\alpha \ll 1$ for normal GAMs, we can solve equations (9*a*)–(9*c*) iteratively to get

$$\delta h_0 = \frac{q_\alpha}{T_{E_\alpha}} J_0\Phi_0 f_{0\alpha} - \frac{\mathrm{i}\omega_\mathrm{d}}{2}\left(\frac{\Phi_{+1}}{\omega - \omega_t} - \frac{\Phi_{-1}}{\omega + \omega_t}\right) \times \frac{q_\alpha}{T_{E_\alpha}} J_0 f_{0\alpha} + \frac{\omega_\mathrm{d}^2}{4\omega}\left(\frac{1}{\omega - \omega_t} + \frac{1}{\omega + \omega_t}\right) \times \frac{q_\alpha}{T_{E_\alpha}} J_0\Phi_0 f_{0\alpha}, \tag{10a}$$

$$\delta h_{\pm1} = \frac{\omega}{\omega \mp \omega_t}\frac{q_\alpha}{T_{E_\alpha}} J_0\Phi_\pm f_{0\alpha} \pm \frac{\mathrm{i}\omega_\mathrm{d}}{2(\omega \mp \omega_t)} \times \frac{q_\alpha}{T_{E_\alpha}} J_0\Phi_0 f_{0\alpha}. \tag{10b}$$

Finally, the perturbation of distribution can be written as

$$\delta f_\alpha = \delta h - q_\alpha\delta\Phi(\vec{r}, t)\frac{f_{0\alpha}}{T_{E_\alpha}} - \frac{q_\alpha}{T_{\mu_\alpha}} \times f_{0\alpha}[1 - J_0(k_\perp\rho_\alpha)\mathrm{e}^{-\mathrm{i}\vec{k}_\perp\cdot\vec{\rho}_\alpha}]\delta\Phi(\vec{r}, t), \tag{11}$$

where $\delta h = \delta h_0 + \delta h_{\pm1}$.

In order to use the quasi-neutrality condition to derive the dispersion relation, we need to obtain the densities of particles. The zero-order perturbation of density is

$$\delta n_0 = \iiint \delta f_{\alpha 0} v_\perp \mathrm{d}\phi \mathrm{d}v_\perp \mathrm{d}v_\parallel = -\frac{1}{2}(k_\perp\rho_\alpha)^2 \times \frac{q_\alpha}{T_{E_\alpha}} n_{0\alpha}\Phi_0(\vec{r}, t) + \frac{\mathrm{i}k_r q\rho_\alpha}{2}\frac{q_\alpha}{T_{E_\alpha}} \times n_{0\alpha}[Z_2(\xi_-)\Phi_{+1}(\vec{r}, t) - Z_2(\xi_+) \times \Phi_{-1}(\vec{r}, t)] - \frac{k_r^2 q^2\rho_\alpha^2}{4\xi}\frac{q_\alpha}{T_{E_\alpha}} n_{0\alpha} \times \Phi_0(\vec{r}, t)[Z_3(\xi_-) + Z_3(\xi_+)], \tag{12}$$

where $\xi = qR\omega/v_{T_\alpha}$ is the normalized frequency and $\xi_\pm = \xi \pm M_\mathrm{p}$. We define the poloidal Mach number $M_\mathrm{p} = \hat{v}_\mathrm{E}/v_{T_\alpha}$ to denote the strength of the electric field. The definition of Z_i functions will be given in the appendix. Using the analogical calculation, the first order perturbation of density is

$$\delta n_{\pm1} = -n_{0\alpha}\Phi_{\pm1}\frac{q_\alpha}{T_{E_\alpha}} - \frac{q_\alpha}{T_{E_\alpha}} n_{0\alpha}\Phi_{\pm1}\xi Z_\mathrm{p}(\xi_\mp) \mp \frac{\mathrm{i}k_r q\rho_\alpha}{2}\frac{q_\alpha}{T_{E_\alpha}} Z_2(\xi_\mp) n_{0\alpha}\Phi_0, \tag{13}$$

where Z_p is the plasma dispersion function.

Normally, the ion thermal velocity is much smaller than that of electrons. We assume that $\xi_\mathrm{i} \gg \xi_\mathrm{e} \simeq 0$. Substituting equation (13) into the quasi-neutrality condition of first order, one can obtain

$$\Phi_{\pm1} = \mp\frac{\mathrm{i}qk_r\rho_\mathrm{i}}{2}\frac{Z_2(\xi_\mp)}{1 + \sigma + \xi Z_\mathrm{p}(\xi_\mp)}\Phi_0, \tag{14}$$

where $\sigma = T_{E_\mathrm{i}}/T_{E_\mathrm{e}}$.

Taking equation (14) into the quasi-neutrality condition $q_\mathrm{i}\delta n_0(\mathrm{i}) + q_\mathrm{e}\delta n_0(\mathrm{e}) = 0$, we can get the dispersion relation

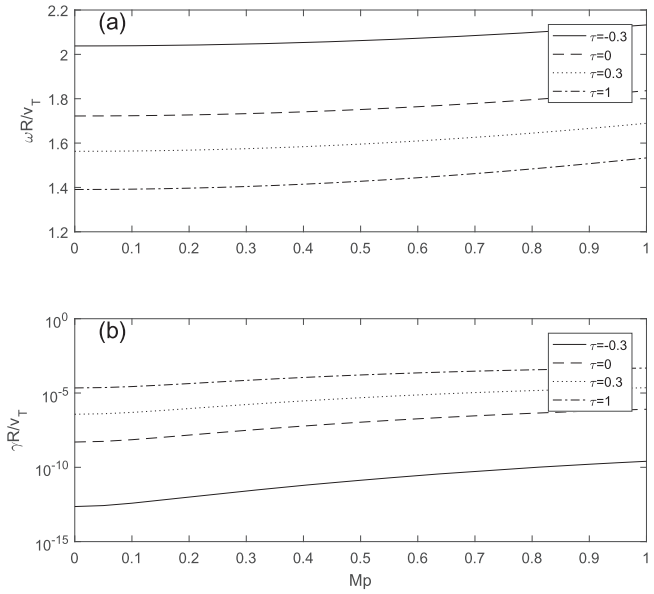

Figure 1. (a) The real frequencies of standard GAMs versus the poloidal Mach number with different value of τ. (b) The damping rates of standard GAMs versus the poloidal Mach number with different value of τ.

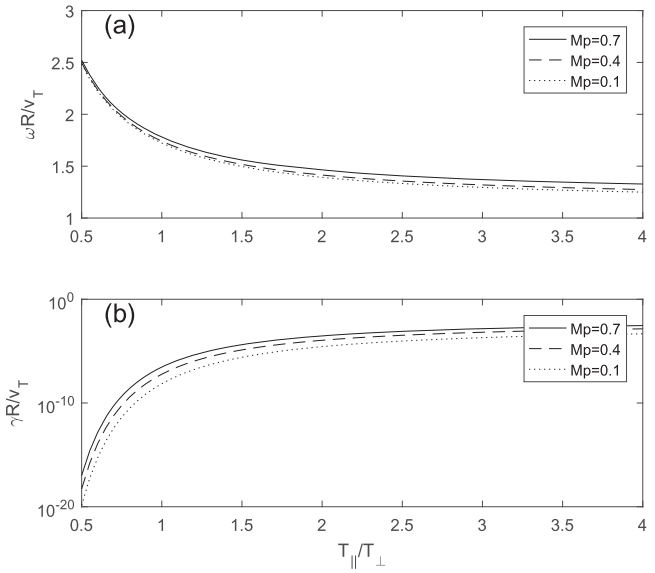

Figure 2. (a) The real frequencies of standard GAMs versus the ratio of the parallel temperature to the perpendicular temperature. (b) The damping rates of standard GAMs versus the ratio of the parallel temperature to the perpendicular temperature.

given by

$$\frac{1}{q^2} - \frac{1}{2}\left[\frac{Z_2(\xi_+)^2}{1+\sigma+\xi Z_p(\xi_+)} + \frac{Z_2(\xi_-)^2}{1+\sigma+\xi Z_p(\xi_-)}\right] + \frac{1}{2\xi}[Z_3(\xi_+) + Z_3(\xi_-)] = 0. \quad (15)$$

Equation (15) is equivalent to the dispersion relation derived in previous works [29] when we drop the anisotropy and the response of electrons for $M_p = 0$. In equation (15), The anisotropic effect is embodied in the Z_i functions. The analysis of the dispersion relation will be given in section 3.

3. Numerical solution to the dispersion relation

It is quite involved to obtain an analytical solution to equation (15), even if approximately for the so-called standard GAM with $|\xi| \gg 1$, using the adiabatic expansion of the plasma dispersion function, as done in previous works [5, 21]. However, it is straightforward to numerically solve the dispersion relation. There exist numerous roots to equation (15) in the complex number domain. We search for the standard GAM solution satisfying $|\xi| \gg 1$ for GAMs are usually detected near the edge of tokamaks where normally $q \gg 1$. It is also the region where poloidal flows and radial electric fields are normally observed [30].

Setting $q = 3$ and $\sigma = 1$, frequencies and damping rates, normalized by the parallel thermal velocity, are plotted versus Mach number for a few τ values in figure 1.

Both frequencies and damping rates increase with respect to the poloidal Mach number. The tendencies are qualitatively in accordance with the previous work [5] where the potential side-band effect was not included. A intuitive explanation for this changing trend with M_p was also given in [15]. In figure 1, the curves of $\tau = 0$ denote the isotropic case. Taking the normal expression of anisotropy, which is indicated by the ratio of the parallel temperature to the perpendicular temperature, we present the frequencies and damping rates varying with respect to the strength of anisotropy in figure 2, with $q = 3$ and $\sigma = 1$.

In figure 2, the real frequencies decrease with the increasing value of the ratio of the parallel temperature to the perpendicular temperature. But the increasing value dramatically promotes the damping rates. When the parallel temperature is lower than the perpendicular temperature, i.e. $T_{||}/T_{\perp} < 1$, the enhanced anisotropy tends to enlarge the real frequency but reduces the damping rate. When the parallel temperature is higher than the perpendicular temperature, the effect is opposite.

From figure 2, we notice that the increasing radial electric field can enhance the real frequency more effectively for the case with the parallel temperature higher than the perpendicular temperature than for the other anisotropic case. While the change of the damping rate versus M_p is not so different for both anisotropic cases.

The changing of the frequency and damping rate versus $T_{||}/T_{\perp}$ is more drastic for smaller $T_{||}/T_{\perp}$. The changing tends to be slow as $T_{||}/T_{\perp}$ get larger than 1.5. Comparing figure 1 with figure 2, we notice that the frequency and damping rate are more sensitive to the ratio of the parallel temperature to the perpendicular temperature. The anisotropy has a stronger impact on standard GAM than that of the radial equilibrium electric field. Since pressure is proportional to temperature, it is qualitatively in agreement with the conclusion of [14], where a fluid model was adopted.

We can give an intuitive interpretation of changing trend of the frequencies and damping rates. Note that the frequencies and the damping rates are normalized by the parallel

thermal velocity. If we fix the parallel temperature and increase the perpendicular temperature, i.e. lowering $T_\parallel/T_\perp$, the ion radial magnetic drift is enhanced. Since the quasi-neutrality condition requires the balance between the radial magnetic drift and the polarization drift, the frequency is then increased to ensure a larger radial polarization drift. The damping results from the transition resonance between the mode and passing ions. If the mode frequency increases, the parallel velocity in resonance with the mode will also increases and the particle number in resonance with the mode will get smaller.

In the above analysis, τ should be larger than -1 to make sure that the perpendicular temperature is positive. It does not matter that T_{μ_i} is negative since it is the parallel temperature and the perpendicular temperature that have physical meanings.

4. Conclusion and discussion

In the present work, the dispersion relation of standard GAMs in tokamak plasmas with anisotropic distribution and a radial equilibrium electric field was derived. The equilibrium distributions of ion and electron are Maxwellian with two temperatures. Dropping the anisotropy and the response of electrons for $M_p = 0$, the previous results could be recovered. We numerically solved the dispersion relation for the standard GAM modes. The frequencies and damping rates increase with the increasing Mach number which denotes the strength of the radial electric field. It is in qualitative agreement with the previous works when the anisotropy is neglected. The profiles of frequencies and damping rates versus the ratio of the parallel temperature to the perpendicular temperature were shown in figure 2. The radial equilibrium electric field has a more important impact on the real frequencies of standard GAMs in the case with the parallel temperature higher than the perpendicular temperature. The increasing ratio of $T_\parallel/T_\perp$ restrains the frequencies of standard GAMs but dramatically promotes the damping rates.

On the whole, the strength of anisotropy has a stronger influence on the frequencies and damping rates than the radial electric field. In experiments, it is possible to control GAMs by using the anisotropic effect. For example, one can decrease the damping rate of GAMs by decreasing $T_\parallel/T_\perp$ through perpendicular heating of ions.

In experiments with high power auxiliary heating, energetic particles may be produced in addition to the anisotropic background. Then EGAMs may be excited. EGAMs is essentially a kind of energetic particle modes with the mode features and mode frequencies determined by the energetic particle distribution. The study of EGAM with anisotropic background distribution may be interesting but not considered in the present work.

The analysis we have done is limited to the standard GAMs with high frequencies and low damping rates, close to the edge of the tokamak. The large aspect ratio circular cross section was assumed in our work, which is only applicable to conventional tokamaks. In recent research, the aspect ratio of tokamaks did also have influence on radial electric field and distribution anisotropy. The flow is stronger and the pressure anisotropy takes a higher value on spherical tokamaks [17]. Further work is necessary to take the device configuration into account in the research of influence of radial electric field and distribution anisotropy. The result is not expected to be changed qualitatively.

Acknowledgments

This work is supported by National Natural Science Foundation of China (Grant No. 11675222). The author appreciates helpful discussions with Dr Yueheng Huang, Baoyi Xie, Xuemei Zhai and Peifeng Fan.

Appendix. Definition of *Z* functions

The plasma dispersion function is

$$Z_p(y) = \frac{\mp 1}{\pi^{1/2}} \int \frac{e^{-x_\parallel^2}}{x_\parallel \pm y} dx_\parallel, \tag{A1}$$

where the integration route is from $-\infty + 0i$ to $+\infty + 0i$ and circumvents the singular point for $\mathrm{Im}(y) \leqslant 0$.

Other Z_i functions are defined as

$$Z_1(\xi) = \frac{1}{\xi\pi^{1/2}} \int \frac{x_\parallel^2 e^{-x_\parallel^2}}{x_\parallel - \xi} dx_\parallel = 1 + \xi Z_p(\xi), \tag{A2}$$

$$\begin{aligned} Z_2(\xi) &= \frac{1}{\pi^{1/2}} \int \frac{x_\parallel^2 + \frac{1}{2(1+\tau)}}{x_\parallel - \xi} e^{-x_\parallel^2} dx_\parallel \\ &= \xi Z_1(\xi) + \frac{1}{2(1+\tau)} Z_p(\xi), \end{aligned} \tag{A3}$$

$$\begin{aligned} Z_3(\xi) &= \frac{1}{\pi^{1/2}} \int \frac{\frac{1}{2(1+\tau)^2} + \frac{1}{1+\tau} x_\parallel^2 + x_\parallel^4}{x_\parallel - \xi} e^{-x_\parallel^2} dx_\parallel \\ &= \frac{1}{1+\tau} Z_2(\xi) + \frac{\xi}{2} + \xi^3 Z_1(\xi). \end{aligned} \tag{A4}$$

References

[1] Diamond P H *et al* 2005 *Plasma Phys. Control. Fusion* **47** R35
[2] Fujisawa A 2009 *Nucl. Fusion* **49** 013001
[3] Tynan G R, Fujisawa A and McKee G 2009 *Plasma Phys. Control. Fusion* **51** 113001
[4] Winsor N, Johnson J L and Dawson J M 1968 *Phys. Fluids* **11** 2448
[5] Zhou D 2015 *Phys. Plasmas* **22** 092504
[6] Zhou D 2016 *Phys. Plasmas* **23** 102503
[7] Wahlberg C 2008 *Phys. Rev. Lett.* **101** 115003
[8] Xie B Y, Guo W F and Xiang N 2017 *Phys. Plasmas* **24** 052510
[9] Itoh K, Hallatschek K and Itoh S I 2005 *Plasma Phys. Control. Fusion* **47** 451
[10] Chakrabarti N *et al* 2007 *Phys. Plasmas* **14** 052308

[11] Sasaki M *et al* 2009 *Phys. Plasmas* **16** 022306
[12] Silva C *et al* 2016 *Nucl. Fusion* **56** 106026
[13] Zwingmann W, Eriksson L G and Stubberfield P 2001 *Plasma Phys. Control. Fusion* **43** 1441
[14] Pustovitov V D 2010 *Plasma Phys. Control. Fusion* **52** 065001
[15] Ivanov A A *et al* 2015 *Plasma Phys. Rep.* **41** 203
[16] Ren H J 2015 *Phys. Plasmas* **22** 072502
[17] Evangelias A and Throumoulopoulos G N 2016 *Plasma Phys. Control. Fusion* **58** 045022
[18] Heidbrink W W and Sadler G J 1995 *Nucl. Fusion* **35** 243
[19] Nazikian R *et al* 2008 *Phys. Rev. Lett.* **101** 185001
[20] Fu G Y 2008 *Phys. Rev. Lett.* **101** 185002
[21] Berk H L and Zhou T 2010 *Nucl. Fusion* **50** 035007
[22] Qiu Z Y, Zonca F and Chen L 2010 *Plasma Phys. Control. Fusion* **52** 095003
[23] Sasaki M *et al* 2016 *Phys. Plasmas* **23** 102501
[24] Elfimov A G, Galvão R M O and Sgalla R J F 2011 *Plasma Phys. Control. Fusion* **53** 105003
[25] Kurki-Suonio T, Lashkul S I and Heikkinen J A 2002 *Plasma Phys. Control. Fusion* **44** 301
[26] Zhou D 2010 *Phys. Plasmas* **17** 102505
[27] Lakhin V P and Ilgisonis V I 2011 *Phys. Plasmas* **18** 092103
[28] Catto P J, Tang W M and Baldwin D E 1981 *Plasma Phys.* **23** 639
[29] Gao Z *et al* 2006 *Phys. Plasmas* **13** 100702
[30] Kobayashi T *et al* 2014 *Nucl. Fusion* **54** 073017